Time Allocation Committee for
MPG time at the ESO 2.2m-telescope
c/o MPI für Astronomie
Königstuhl 17
D-69117 Heidelberg / Germany

Application No.	
Observing period	October 2020
Received	

APPLICATION FOR OBSERVING TIME

from [X] MPIA [ ] MPG institute [ ] other

1. Telescope: 2.2-m [X]

2.1 Applicant

Mrs. Sarah **Gebruers**	MPIA & IoA, KU Leuven
Name	Institute
Königstuhl 17	D-69117 Heidelberg
street	ZIP code - city
sarahg	sarah.gebruers@kuleuven.be
ESO User Portal username	e-mail

2.2 Collaborators

J. Mombarg & S. Garcia & T. Van Reeth	Institute of Astronomy, KU Leuven
name(s)	institute(s)
A. Tkachenko, C. Aerts & H. -W. Rix	Institute of Astronomy, KU Leuven & MPIA
name(s)	institute(s)

2.3 Observers

J. Mombarg	S. Garcia
name	name

By specifying the names under item 2.3 it is obligatory to also send out these observers to La Silla, if required. Correspondence on the rating of this application will be sent to the applicant (P.I.) as quoted under 2.1 above.

3. Observing programme: Category: E

Title : **Atomic diffusion in A/F-stars with TESS+FEROS asteroseismology**

Abstract : State-of-the-art stellar evolution models are still lacking quantitative physics descriptive for the transport of chemical elements. Microscopic atomic diffusion must occur inside stars and we aim to constrain it through its effect on surface abundances and stellar oscillations. This requires high-resolution and high-S/N FEROS spectra to derive precise atmospheric parameters (T_{eff}, log g and surface abundances) for A/F-type stars that allow optimal asteroseismic modelling with unprecedented TESS data. The proposed TESS sample is much brighter and complementary in metallicity to the existing Kepler sample. This provides us with the unique opportunity to probe the influence of metallicity and address the role of chemical composition in atomic diffusion and mode excitation.

4. Instrument: [ ] WFI [X] FEROS [ ] GROND

5. Brightness range of objects to be observed: from 7.5 to 10.3 V-mag

6. Number of hours:

applied for			already awarded	still needed
26.5			none	none
no restriction	grey	dark		

7. Optimum date range for the observations: .... 01.10.2020 – 31.03.2021
Usable range in local sideral time LST: .... 0:50h – 10:50h

Astrophysical context

Asteroseismology is the study of stellar oscillations either restored by the pressure force (p modes) or the buoyancy and Coriolis force (g modes). It has brought an entirely new look on the interior rotation and mixing in low- and intermediate mass stars. In the *Kepler* data, unanticipated discrepancies between theoretically predicted and observed oscillations are present (e.g. [1]). Transport of chemical elements is challenging to quantify because it is model-dependent and involves the estimation of several correlated free parameters. The lack of well-calibrated element transport processes already affects the core-hydrogen burning stage and remains throughout stellar evolution (e.g. [2]). Recent studies based on *Kepler* data of low-mass stars revealed that atomic diffusion is a necessary ingredient in stellar models to explain the observed signature of p-mode glitches due to He settling at the base of the outer convection zone [3]. Moreover, it was found that mixing due to atomic diffusion (including radiative levitation) is at least as important as macroscopic rotational mixing for slow and moderate rotators with $M \in [1.4,\, 1.5]\,\mathrm{M}_\odot$ [4].

We aim to improve the theory of chemical element transport for stars with $M \in [1.3,\, 2.0]\,\mathrm{M}_\odot$ in their longest lasting phase: core-hydrogen burning. *We will investigate the importance of microscopic atomic diffusion in these stars by performing overarching asteroseismic, astrometric, and spectroscopic modelling of element mixing, including radiative levitation.* All stars in our sample lie in the TESS Southern Continuous Viewing Zone (S-CVZ). The 1-yr TESS photometry provides us with a high frequency precision (~ 0.002 d^{-1}) necessary to detect gravity-mode period spacing patterns, which form the input for asteroseismic modelling. An example of such a pattern for a star in our sample is shown in Fig. 1. FEROS is an optimally suited instrument to obtain high-S/N spectra for these pulsating TESS stars, which is crucial for asteroseismic modelling that is otherwise prone to degeneracies.

Immediate aim

The FEROS spectrograph is ideal to acquire high-resolution ($R >$ 40000), high-S/N ($\geq$ 200) spectra for our sample of 35 pulsating A/F stars. High resolution is required to resolve individual lines of possible slow rotators among the targets. The spectra will be used to derive radial velocities (to detect binaries), stellar parameters and surface abundances. T_{eff} and log g are paramount to lift a large part of the degeneracies in asteroseismic modelling (e.g. [5]). Furthermore, when atomic diffusion is included into the stellar models, predictions about the surface abundances can be made once the age of the star is known. Comparing these predictions with abundances derived from high-S/N FEROS spectra will allow us to constrain any missing mixing processes in the radiative region of the star.

Previous work

The *Kepler* mission allowed to study the interior rotation of $\sim$700 A/F-type gravity-mode pulsators [6]. For only $\sim$40 of them, high-resolution spectroscopy could be obtained due to their faintness. This spectroscopy combined with *Kepler* data allowed to derive the near-core rotation rate [7] and chemical mixing [5] from period spacing patterns (Fig. 1). The TESS mission is now delivering the same probing power for much brighter pulsating A/F stars in the S-CVZ, that have different metallicities compared to those observed by *Kepler*. This will allow us to study the influence of metallicity on the chemical stratification caused by microscopic atomic diffusion. The effect of atomic diffusion on g modes has so far been investigated for only two g-mode pulsators (by us, see [8]). This proof of concept shows the inferred stellar mass and age change significantly (up to 12% in mass and 50% in age) depending on whether or not atomic diffusion is included in the models. Moreover, [8] have demonstrated that observed surface abundances in combination with pulsation frequencies have the potential to infer whether any additional mixing processes are at work (Fig. 2).

Layout of observations

We analyzed 8712 A- and F-type stars in the S-CVZ of which 35 are bright (Vmag $<$ 10.3) stars for which clear g-mode period spacing patterns are detected. To derive surface abundances (H, He, C, Na, Mg, Si, Ca, Fe and Ni) for this subset with a high enough precision to constrain atomic diffusion (see Fig. 2) and determine T_{eff}/log g with a precision of $<$ 5%/0.20 dex, a S/N$\,\geq\,$200 is needed (cf. Fig. 3). Furthermore, the detection of stellar pulsations is affected by the potential presence of a companion due to tides. Therefore, we request two epochs of each star, maximally separated in time, to probe for binarity. Single stars and SB1 systems will be used for our science case by co-adding the two epochs and shifting them to the same RV. SB2 systems will be analysed in a separate project, focusing on tidal asteroseismology, for which additional future spectra may be needed.

Strategic importance for MPIA

The proposed project is part of a strategic collaboration on stellar physics between MPIA and KU Leuven. CA has recently been appointed as an external MPS member, and **the PI has taken up a joint PhD position between these two departments. The requested data in this proposal is crucial for the PI's PhD research** which requires spectroscopic parameters for asteroseismic modelling. *With this project we will improve state-of-the-art stellar evolution models, which is particularly important for galactic evolution, as the mixing in the stellar interior dictates a star's lifetime, and thereby, the chemical feedback.*

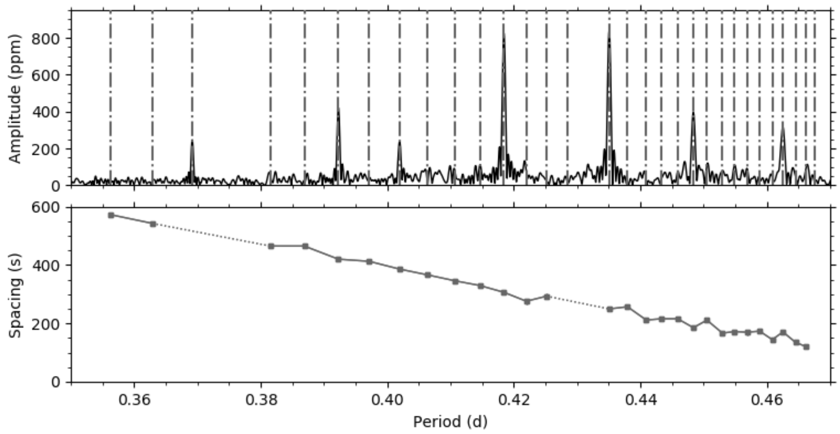

Fig. 1: *Top*: Fourier spectrum of the F-type star HD 272099 pulsating in g modes from TESS photometry. *Bottom*: Spacing between periods of consecutive radial order (same surface geometry) versus period. Missing periods between spacings are indicated with dotted lines.

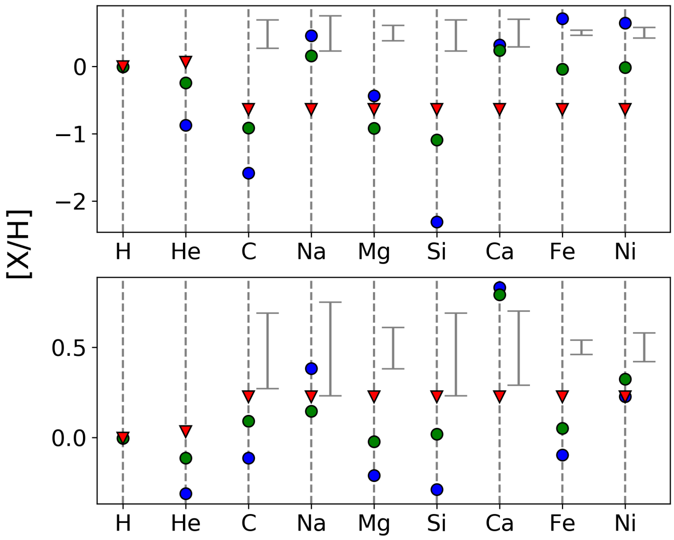

Fig. 2: Predicted surface abundances [X/H] for a star with $M = 1.4\,\mathrm{M}_\odot$,$Z_{\rm ini} = 0.003$ (*top panel*) and a star with $M = 1.9\,\mathrm{M}_\odot$,$Z_{\rm ini} = 0.022$ (*bottom panel*). Red triangles: model without atomic diffusion; blue/green dots: model with atomic diffusion for 60% and 30% of the initial hydrogen mass fraction left in the core, respectively. No additional mixing processes have been added, hence, the surface abundances for the model without atomic diffusion remain constant throughout the main sequence. Typical errors on the measured abundances for a *Kepler* g-mode pulsator obtained from S/N ≈100 spectra taken with the HERMES spectrograph at the Mercator telescope on La Palma (grey error bars) are too large to derive the envelope mixing profile; to achieve this, a twice as high S/N is needed.

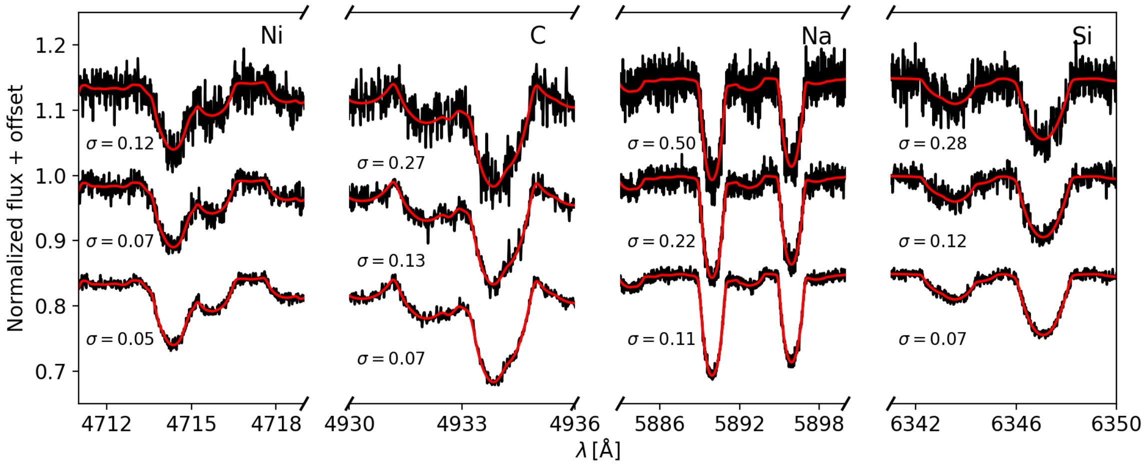

Fig. 3: Synthetic spectra of a $T_{\rm eff} = 7000\,\mathrm{K}, \log g = 3.0$, F star with S/N ratios of 50 (top), 100 (middle) and 200 (bottom) zoomed in on lines of Ni, C (4932 Å), Na and Si. The spectrum without noise added is plotted in red. Below each spectrum, the resulting precision on the surface abundances ([X/H]) is indicated. To obtain the necessary precision dictated by Fig. 2 for all stars in our sample, S/N ≈ 200 is needed.

9. Objects to be observed

(Objects to be observed with high priority should be marked in last column)

Designation	α (2000)	δ (2000)	magnitude in spectral range to be observed	priority
HD 43199	$06^h\,10^m\,52\overset{s}{.}8907$	$-61°\,29'\,59''3165$	7.5	1
HD 53144	$06^h\,54^m\,03\overset{s}{.}5473$	$-77°\,46'\,50''7053$	7.5	1
HD 61314	$07^h\,31^m\,12\overset{s}{.}2458$	$-74°\,41'\,27''5865$	7.6	1
HD 28201	$04^h\,21^m\,26\overset{s}{.}733$	$-69°\,36'\,56''4265$	8.4	1
HD 30131	$04^h\,41^m\,02\overset{s}{.}6767$	$-60°\,50'\,45''0752$	8.5	1
HD 38992	$05^h\,45^m\,12\overset{s}{.}3415$	$-62°\,55'\,00''7757$	8.7	1
HD 45873	$06^h\,26^m\,06\overset{s}{.}4638$	$-60°\,15'\,29''1808$	8.8	1
HD 60101	$07^h\,28^m\,37\overset{s}{.}2452$	$-64°\,38'\,11''6153$	8.9	1
HD 45986	$06^h\,25^m\,18\overset{s}{.}1515$	$-67°\,29'\;\;37''067$	9.1	1
HD 56027	$07^h\,08^m\,43\overset{s}{.}5113$	$-72°\,18'\;\;43''99$	9.2	1
HD 37897	$05^h\,38^m\,14\overset{s}{.}795$	$-57°\,12'\,27''4944$	9.2	1
HD 41686	$06^h\,02^m\,29\overset{s}{.}3525$	$-61°\,42'\,47''7396$	9.3	1
HD 28223	$04^h\,22^m\,35\overset{s}{.}9829$	$-65°\,43'\;\;57''844$	9.3	1
HD 48817	$06^h\,40^m\,52\overset{s}{.}9462$	$-63°\,06'\,49''8676$	9.4	1
HD 56025	$07^h\,11^m\,20\overset{s}{.}4238$	$-61°\,49'\,43''4336$	9.5	1
HD 32955	$05^h\,02^m\,56\overset{s}{.}164$	$-60°\,40'\,42''7887$	9.6	1
HD 38281	$05^h\,40^m\,19\overset{s}{.}2059$	$-62°\,38'\,51''7744$	9.7	1
HD 28341	$04^h\,23^m\,08\overset{s}{.}0236$	$-67°\,52'\,52''9884$	9.8	1
CD-56 1104	$05^h\,06^m\,57\overset{s}{.}4491$	$-56°\,26'\,02''5446$	9.8	1
HD 64700	$07^h\,50^m\,42\overset{s}{.}0828$	$-65°\,53'\,16''1787$	9.8	1
CD-63 160	$04^h\,42^m\,36\overset{s}{.}7475$	$-62°\,57'\,38''0498$	9.9	1
CPD-63 540	$06^h\,17^m\,36\overset{s}{.}0824$	$-63°\,16'\,58''4369$	10.0	1
HD 272099	$06^h\,14^m\,28\overset{s}{.}1683$	$-72°\,04'\,43''3321$	10.0	1
CD-65 448	$06^h\,38^m\,53\overset{s}{.}3603$	$-65°\,58'\,37''1087$	10.2	1
CD-71 206	$04^h\,11^m\,24\overset{s}{.}8922$	$-71°\,08'\,00''2304$	10.2	1
CPD-62 550	$05^h\,57^m\,47\overset{s}{.}2942$	$-62°\,04'\,57''6132$	10.3	1
HD 47545	$06^h\,34^m\,46\overset{s}{.}9294$	$-63°\,15'\,43''6941$	7.8	2
HD 26733	$04^h\,08^m\,30\overset{s}{.}6723$	$-68°\,42'\,08''0556$	8.4	2
HD 57723	$07^h\,15^m\,41\overset{s}{.}4901$	$-72°\,44'\,28''9601$	8.4	2
HD 51997	$06^h\,54^m\,11\overset{s}{.}3358$	$-68°\,09'\;\;29''034$	8.6	2
HD 48247	$06^h\,37^m\,05\overset{s}{.}3164$	$-67°\,28'\,08''5448$	8.6	2
HD 62363	$07^h\,37^m\,57\overset{s}{.}8888$	$-70°\,04'\,05''3018$	8.7	2
HD 311331	$07^h\,43^m\,41\overset{s}{.}1871$	$-72°\,28'\,28''4849$	9.7	2
CD-60 1503	$06^h\,36^m\,19\overset{s}{.}9651$	$-60°\,44'\;\;49''659$	10.1	2
TIC141153472	$05^h\,22^m\,45\overset{s}{.}5452$	$-75°\,43'\,01''3134$	10.2	2

10. `Justification of the amount of observing time requested:`

The science goals of our proposal require a high-resolution ($R > 40000$) instrument covering a large wavelength range in order to measure several Balmer lines and the optical transitions of various metals. This makes FEROS the ideal instrument. Our target list consists of all bright (Vmag < 10.3) A- and F-type g-mode pulsators in the Southern CVZ of TESS, i.e. stars that show g-mode period spacing patterns, and can thus be asteroseismically modelled. The sample we propose here comprises 35 stars, which is of similar size compared to the *Kepler* sample, allowing for a rigorous comparison between the two samples. Moreover, previous asteroseismic studies have demonstrated that a sample ∼40 stars is sufficient to meet the science goal of this proposal (see [7] and [5]). We have cross-matched our list with the ESO archive, but there are no spectra available for any of the stars we propose. Therefore, we request two spectra for each star in the sample, maximally separated in time within the semester to detect possible binaries with short and/or intermediate periods. The targets are prioritised according to the quality of the detected g-mode period spacing patterns. Stars with priority 1 have a clear period spacing pattern, while for stars with priority 2 more TESS photometry data is needed to improve the period spacing pattern. These additional data will be obtained when TESS turns back to the Southern Hemisphere in the third year of the mission, starting July 2020.

We require a S/N ≥ 150 at 5000 Å per spectrum to meet our science goals when combining the two epochs, i.e., for a S/N ≥ 200. Based on the FEROS Exposure Time Calculator, this would require an exposure time of 540 sec for a star with Vmag = 9.0 (seeing ≤ 1.3″). The exposure time for a star in the V-mag range between 7.5 and 10.3 mag is then rescaled by $10^{((\mathrm{Vmag}_i - 9.0)/2.5)} \cdot 540\,\mathrm{sec}$ + overhead. The total overhead per target is 570 sec, including 1) 360 sec for the telescope pointing, target acquisition and centering on fibre; 2) 60 sec for the FCU + Adapter setup; 3) 150 sec for slow, high-gain read-out (FEROS User Manual, Issue 78.0, Date 15/10/2006). Therefore, the total amount of time requested for this program is **26.5 hours** (including the 2 epochs per target).

11. `Constraints for scheduling observations for this application:`

Individual visits should be maximally separated within the observing semester to increase the detection probability of both short- and intermediate-period binaries.

12. `Observational experience of observer(s) named under 2.3:`
`(at least one observer must have sufficient experience)`

All observers listed have ample experience in high-resolution spectroscopy with FEROS and/or with the HERMES spectrograph attached to the 1.2-m Leuven Mercator telescope at La Palma Observatory, whose design and use is based on the FEROS spectrograph.

13. `Observing runs at the ESO 2.2m-telscope (preferably during the last 3 years)`
`and publications resulting from these`

Telescope	instrument	date	hours	success rate	publications
2.2m	FEROS	Dec 2019	122.5		Data analysis ongoing
This was the first KU Leuven FEROS run in the context of asteroseismology. The project focused on OB type stars to investigate angular momentum transport. The data were obtained in December 2019 and February 2020 and are currently being reduced and analysed by CA's team, including the PI.					

14. References for items 8 and 13:

[1] Aerts, C.; Mathis, S.; Rogers, T. M., 2019, *Angular Momentum Transport in Stellar Interiors*, ARAA, 57, 35

[2] Dotter, A.; Conroy, C.; Cargile, P.; Asplund, M., 2017, *The Influence of Atomic Diffusion on Stellar Ages and Chemical Tagging*, ApJ, 840, 99

[3] Verma, K.; Raodeo, K.; Basu, S.; et al., 2019, *Helium abundance in a sample of cool stars: measurements from asteroseismology*, MNRAS, 483, 4678

[4] Deal, M.; Goupil, M. -J.; Marques, J. P.; Reese, D. R.; Lebreton, Y., 2020, *Chemical mixing in low mass stars. I. Rotation against atomic diffusion including radiative acceleration*, A&A, 633, A23

[5] Mombarg, J. S. G.; Van Reeth, T.; Pedersen, M. G.; Molenberghs, G.; Bowman, D. M.; Johnston, C.; Tkachenko, A.; Aerts, C., 2019, *Asteroseismic masses, ages, and core properties of γ Doradus stars using gravito-inertial dipole modes and spectroscopy*, MNRAS, 485, 3248

[6] Li, G.; Van Reeth, T.; Bedding, T. R.; Murphy, S. J.; Antoci, V., Ouazzani R.-M.; Barbara, N. H., 2020, *Gravity-mode period spacings and near-core rotation rates of 611 γ Doradus stars with Kepler*, MNRAS, 491, 3586

[7] Van Reeth, T.; Tkachenko, A.; Aerts, C., 2016, *Interior rotation of a sample of γ Doradus stars from ensemble modelling of their gravity-mode period spacings*, A&A, 593, A120

[8] Mombarg, J. S. G.; Dotter, A.; Van Reeth, T.; Tkachenko, A.; Gebruers, S.; Aerts, C., *Asteroseismic modeling of gravity modes in slowly rotating A/F stars with radiative levitation*, accepted for publication in ApJ, arXiv:2004.13037

Tolerance limits for planned observations:

maximum seeing:	2.5″	**minimum transparency:**	50%	**maximum airmass:**	2.0
photometric conditions:	no	**moon: max. phase / ∠ :**	0.8/30°	**min. / max. lag:**	30/60 nights